Study of the Kinetics of Glass Alteration by Small-Angle X-ray Scattering

Lorette Sicard,[†] Olivier Spalla,*[,†] and Philippe Barboux[‡]

CEA Saclay, DSM/DRECAM/Service de Chimie Moléculaire, 91191 Gif sur Yvette Cedex, France and Laboratoire de Physique de la Matière Condensée, CNRS UMR 7643C, Ecole Polytechnique, 91128 Palaiseau Cedex, France

Received: January 19, 2004; In Final Form: April 2, 2004

The alteration in water of homogeneous sodium borosilicate glasses containing different concentrations of zirconium has been studied. The dissolution kinetics were followed by chemical analysis, and the morphology of the interfacial altered layer was studied by small-angle X-ray scattering (SAXS). Two types of dissolution behaviors have been observed, depending on the initial concentration of zirconium in the glass. Below 2% ZrO_2, the glass dissolves with a constant thickness of the altered layer (i.e., the leaching of the elements of the glass causes a shrinkage of the particle size). Above 2% ZrO_2, the skeleton of the altered layer becomes less soluble; consequently, the alteration is isovolumic with an altered layer thickness increasing with time. Whatever the zirconium content, the altered layer initially presents a large porosity associated with a high specific surface area. Then, the dissolution and recondensation of silica cause a ripening of the pores with a decrease of the specific surface area. Zirconium strongly modifies the dissolution kinetics and also the morphology of the altered layer. It increases the specific area of the altered layer, which delays the formation of a passivating layer at the glass−water interface. As a result, small amounts of zirconium lead to larger alteration depths.

1. Introduction

The contact of glass with water results in an alteration of its surface. Many studies have been devoted to the understanding of the mechanisms involved in this corrosion effect. Indeed, the durability of glass is of prime importance in many fields from everyday life to specific applications. The most common effect is a change in the visual appearance of soda-lime glasses after repeated cleaning cycles.[1,2] The problem also concerns the aging of stained glass windows in cathedrals[3] and the corrosion of glass fibers (optical as well as insulating). The long-term alteration of basaltic glasses[4,5] and their geological transformation are also considered. Finally, the objective in the nuclear industry is to ensure that the nuclear waste glasses retain, as long as possible, the radioactive elements that they contain. In this particular field, we want to understand the alteration in water of sodium borosilicate glasses, and we study the effect of elements of low solubility on the alteration mechanism. In particular, zirconium, which was chosen for this work, is known to increase the glass durability in water above pH 7. At the same time, it can be considered to be a nondangerous (although fair) analogue to nuclear elements (Pu, U, Th).

Most of the studies in the literature[6−8] are devoted to the kinetics of leaching of the different glass components. These studies have identified several steps in the corrosion process. The initial step corresponds to interdiffusion (exchange between the protons contained in water and sodium cations), which predominates in the short term. The following step corresponds to the congruent dissolution of all of the elements. Then, under static conditions (closed systems), a decrease of the alteration rate is observed. The dissolution becomes incongruent, and a superficial porous layer forms. Finally, the alteration nearly stops. Two explanations have been proposed for this last step: either a thermodynamic equilibrium between the thermodynamic activities of the silicon contained in the glass and that dissolved in solution[9] or the formation of a protective layer.[8] To examine this second explanation, many studies have focused on the characterization of this superficial layer (by FTIR, NMR, TEM, AFM, XPS, SIMS, etc.), in parallel to the analysis of the solution.[8,10,11] For example, atomic force microscopy[10] was recently used to quantify the shrinking or swelling of these alteration layers. Simulations have also been carried out to characterize the morphology of the altered layer.[12]

Knowledge of the porous structure of the layer is essential, from a practical point, to determine if the altered layer actually constitutes a barrier to further alteration. From a fundamental point of view, it is also interesting to understand how a sharp interface is transformed to a porous one as an equilibrium or a metastable end-product.[13] Very few kinetics studies have coupled the morphology of the corrosion layer with the chemical reaction. The porosity of the altered layer has been already studied by gas adsorption.[14] However, this technique requires a preliminary drying of the sample that may corrupt the porosity through the effect of capillary forces during the removal of water. On the contrary, small-angle X-ray scattering (SAXS) measurements have been revealed to be an efficient way to quantify the porosity in glasses,[15−17] even in situ during the alteration.[16,17] Previous studies[16,17] have focused on the development of a SAXS methodology to determine the morphological properties of the altered layer (volume of the altered layer, specific surface area and porous volume of this layer, dissolution of the grain envelope) quantitatively. In this paper, the chemical aspects of the leaching and the short-term kinetics in relation with the morphology will be emphasized.

* Corresponding author. E-mail: spalla@drecam.saclay.cea.fr. Tel: 33 1 69 08 67 43. Fax: 33 1 69 08 66 40.
[†] CEA Saclay.
[‡] Ecole Polytechnique.

10.1021/jp049727q CCC: $27.50
Published on Web 05/12/2004

TABLE 1: Molar Composition of the Pristine Glasses

reference	% SiO_2	% Na_2O	% B_2O_3	% ZrO_2
0% ZrO_2	0.7	0.15	0.15	0.000
0.5% ZrO_2	0.697	0.149	0.149	0.005
1% ZrO_2	0.693	0.149	0.149	0.010
2% ZrO_2	0.686	0.147	0.147	0.020
5% ZrO_2	0.667	0.143	0.143	0.048
10% ZrO_2	0.636	0.136	0.136	0.091

2. Experimental Section

2.1. Glasses. The alterations were performed on powders to produce a large amount of the altered layer. The glasses used in this work contained SiO_2, B_2O_3, Na_2O, and ZrO_2 in molar ratios of 70, 15, 15, and x where x varies from 0 to 10. Their compositions are given in Table 1. To simplify the notation, x will be ascribed to the molar percentage of zirconia in the following text. However, the true percentages are actually $x/(100 + x)$. The Na_2O, B_2O_3, SiO_2 composition has been chosen in the homogeneous part of the phase diagram.[18] The addition of ZrO_2 does not affect the glass homogeneity as shown by the optical transparency and, at the microscopic scale, by small-angle X-ray scattering as discussed below.

The oxide powders (SiO_2 (Prolabo), H_3BO_3 (Prolabo), Na_2CO_3 (Strem Chemicals), ZrO_2 (Prolabo)) were mixed together and heated in a platinum crucible at 800 °C for 2 h and then at 1350 °C for 4 h. Finally, they were poured onto a graphite plate at room temperature. The chemical composition, as determined by chemical analysis, shows a slight evaporation of Na and B but does not vary by more than 1% from the initial composition.

The resulting glasses were crushed and sieved through a multiple stage column of filters. The powders were then washed in an ultrasonic bath containing acetone to get rid of the finer particles that can be left at the glass surface. In this paper, only the results obtained for particles in the size range from 32 to 50 μm are reported.

2.2. Alteration Procedure. The particles were altered under static conditions. Glass powder (300 mg, specific surface area of 0.3 m^2/g) was added to 50 mL of deionized water. This corresponds to a glass surface-to-solution volume ratio (S_0/V_{sol}) of 2000 m^{-1}. The kinetics were carried out at 90 °C for times ranging from 1 day up to 4 months.

2.3. Chemical Analysis. Silicon and boron concentrations in solution were determined with colorimetry kits using a WTW (Wissenschaftlich-Technische Werkstatten GmbH) Photolab S12 spectrophotometer. For silicon, the solutions were first diluted and heated overnight at 90 °C before the titration in order to dissolve the colloidal particles that could have formed. Sodium concentrations were measured by flame spectroscopy absorption. The accuracy of the analysis is 10% for the three elements.

From the chemical analysis, a leached fraction LF(j) of each element j could be calculated. It is defined by the ratio between the extracted mass of j and the initial mass of this element in the pristine glass:

$$LF(j) = \frac{c_j \times V_{sol}}{f_j \times m_0} \quad (1)$$

where c_j is the concentration of element j in the solution of volume V_{sol}, f_j is the weight fraction of element j, and m_0 is the initial mass of glass. The maximum value of the leached fraction of element j will be noted as LF*(j).

2.4. SAXS Experiments. SAXS experiments were performed either at the European Synchrotron Radiation Facility (ESRF) in Grenoble (for alteration times of more than 2 weeks) or at the Commissariat à l'Energie Atomique (CEA) in Saclay (for short alteration times up to 1 week). In the first case, the energy chosen was 17 717 eV ($\lambda = 0.70$ Å). The scattering patterns were recorded at two different sample−detector distances (2.225 and 0.570 m) to have an accessible q range between 0.004 and 0.7 $Å^{-1}$. In the second case, the patterns were recorded on two laboratory-made instruments using the same rotating Cu anode producing photons at $\lambda = 1.54$ Å.[19,20] This allows us to obtain the scattering curves over a wide q range (between 0.0003 and 0.5 $Å^{-1}$), where q is defined from the scattered angle θ by $q = (4\pi \sin(\theta/2))/\lambda$. In all cases, the samples were analyzed without drying. For this purpose and to avoid sedimentation, a small amount of wet glass powder was mixed with a 1 wt % xanthan solution. The resulting gel was then transferred to a cell sealed with two Kapton sheets. The contribution of the cell windows was subtracted. The signal arising from xanthan is negligible.

The intensity $I_1(q)$ per volume unit of solid has been calculated using eq 2, established in a previous study:[21]

$$I_1(q) = \frac{I(q)}{\Phi_s} = \frac{1}{\Phi_s T e N_0} \frac{\Delta N}{\Delta \Omega} \quad (2)$$

where $I(q)$ is the intensity scattered per unit volume of sample, Φ_s is the total volume fraction of solid, ΔN is the flux of photons scattered in the solid angle $\Delta\Omega$, N_0 is the total incident flux of photons on the sample, T is the transmission, and e is the thickness of the sample. Φ_s is calculated by weighing the mixture of wet glass and xanthan solution before and after drying at 70 °C. The thickness e is deduced from the measurement of the transmission by eq 3:

$$e = \frac{-\ln(T)}{(1 - \Phi_s)\mu_w + \Phi_s \mu_s} \quad (3)$$

where μ_w and μ_s are the absorption coefficients of water and of the dried solid, respectively.

3. Results

3.1. Leaching of the Elements. The concentration and the leached fractions (LF) of silicon, sodium, and boron allow us to follow the degree of alteration of the glass particles. The amount of dissolved zirconium is negligible at the pH of the experiment (between 8 and 10). The evolution of LF(Si), LF(Na), and LF(B) is drawn as a function of the alteration time for the glasses containing 0% ZrO_2 (Figure 1a), 1% ZrO_2 (Figure 1b), and 5% ZrO_2 (Figure 1c). The plot of the leached fraction was preferred because it better allows us to compare the extracted percentage of each element for a given composition. The leached fractions of boron and sodium are very similar, in all cases, even if the curve representing LF(B) is slightly higher than the one representing LF(Na). At the pH of the solution, boron and sodium are far from saturation, and the pH of the solution is fixed by the dissolved sodium and borate ions. On the contrary, the silica concentration corresponds to a saturation value. It is nearly equal to 400 ppm for the glasses containing up to 1% ZrO_2, similar to the saturation concentration of amorphous silica at such pH values. For the glasses containing more ZrO_2, the concentration of silicon at saturation strongly decreases. The incongruent leaching of boron and sodium as compared to that of silicon creates a porosity within the altered layer. The leaching of silicon can either create more porosity or lead to a total dissolution of the external part of the glass, resulting in a decrease of the particle size.

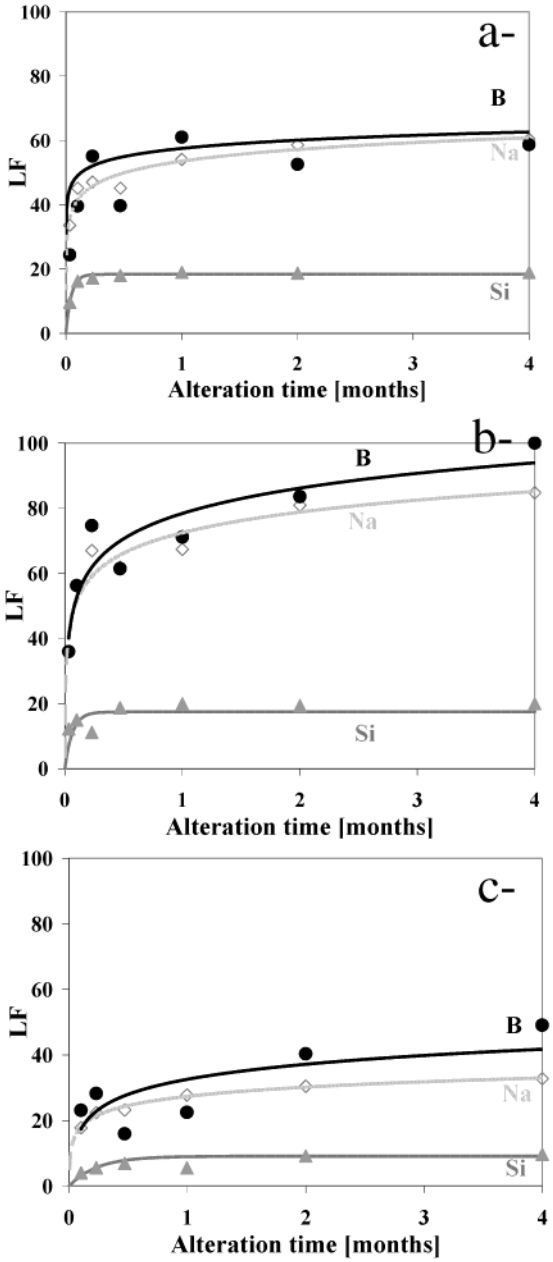

Figure 1. Leached fractions (LF) of B (in black), Na (in pale gray), and Si (in dark gray) vs the alteration time for the glasses containing (a) 0% ZrO_2, (b) 1% ZrO_2, and (c) 5% ZrO_2. For Si, the lines correspond to fits with a first-order kinetics law. In the case of Na and B, they are just a guide for the eye.

Qualitatively, the curves obtained for the different cations can be described in a similar way, whatever the zirconium content. They are characterized by a steep increase during the first day of alteration. Then, the leaching slows down until reaching a plateau. However, the addition of zirconium has a quantitative effect on the alteration of the glasses in two aspects: the kinetics of alteration and the alteration degree at saturation (when the concentrations of the different cations in solution remain constant).

First, zirconium has a drastic impact on the kinetics of leaching. It can be clearly seen on the curves of LF(B) and LF(Na) as well as those of LF(Si). The time required to reach saturation and the end of the dissolution increases with zirconium content. It is 7 days for the glass containing no ZrO_2, whereas it is more than 1 month for the glass with 5% ZrO_2. The curves obtained for Si can be fit by a first-order kinetic law of the form[8] $C(t) = C_\infty(1 - \exp(-t/\tau))$. The results are given in Table 2 and represented on Figure 1. The decrease of τ confirms the slowing of the alteration kinetics with the addition of zirconium. However, the data are only qualitative because the fits are very fair in these experiments performed in unbuffered solutions with changes in pH associated with the release of sodium and borate ions. A first order kinetic law does not work for Na and B.

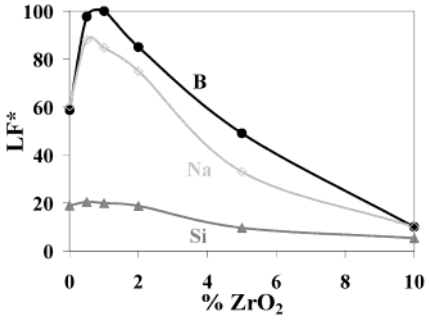

Figure 2. Leached fractions of B (in black), Na (in pale gray), and Si (in dark gray) after 4 months of alteration (LF*) as a function of the ZrO_2 concentration.

TABLE 2: pH and Results of the Fits of the LF(Si) Curves by a First-Order Kinetics Law of the Type $LF(t) = LF_\infty(1 - \exp(-t/\tau_{Si}))$

reference	pH	LF_∞(Si)	C_∞(Si) [ppm]	τ_{Si} [month^{-1}]
0% ZrO_2	9.5	18.4	360	0.046
0.5% ZrO_2	9.6	19.8	388	0.023
1% ZrO_2	9.7	19.1	374	0.036
2% ZrO_2	9.5	17.4	303	0.064
5% ZrO_2	9.1	9.1	153	0.24
10% ZrO_2	8.7	5.4	83	0.19

Second, the degree of alteration of the glasses differs depending on the amount of zirconium contained in the pristine glass. Figure 2 illustrates this effect. Indeed, the leached fractions of boron, sodium, and silicon at saturation (LF*), after 4 months of alteration, are represented with respect to the ZrO_2 content. At this time, the glasses can be considered to be in their final alteration state. The behaviors of silicon and of the most soluble elements (Na and B) must be distinguished. Indeed, LF*(Si) is similar for all of the glasses containing less than 2% ZrO_2 (LF*(Si) $\approx$ 20%). When adding more than 2% ZrO_2, the leached fraction of silicon drops (LF*(Si) $\approx$ 10% for glasses containing 5 and 10% ZrO_2). Concerning boron and sodium, a decrease of LF* is also observed when increasing the zirconia concentration from 2 to 10%, but the addition of less than 2% ZrO_2 results in an increase of the maximum of alteration, LF*: LF*(B) is equal to 60% when the glass does not contain zirconium, whereas all of the boron content is leached for glasses containing 0.5 to 1% zirconia.

The results obtained for ZrO_2 content above 2% were expected. The low solubility of Zr at this pH may be associated with a very low dissolution (hydrolysis rate) of the Si−O−Zr bonds or to an even faster recondensation rate and reprecipitation of zirconium oxo-hydroxide species. The solubility of the silicon atoms linked to a zirconium atom may become very low. Thus, LF*(Si) is expected to decrease; consequently, the intrusion of water into the glass would become more difficult, resulting in a decrease of LF*(B) and LF*(Na). The first part of the curve, below 2% ZrO_2, is more surprising. Moreover, the comparison of the behaviors of the glasses containing 2% ZrO_2 with the Zr-free glass is interesting. Indeed, more boron is extracted from the glass containing ZrO_2 than from the Zr-free glass, whereas

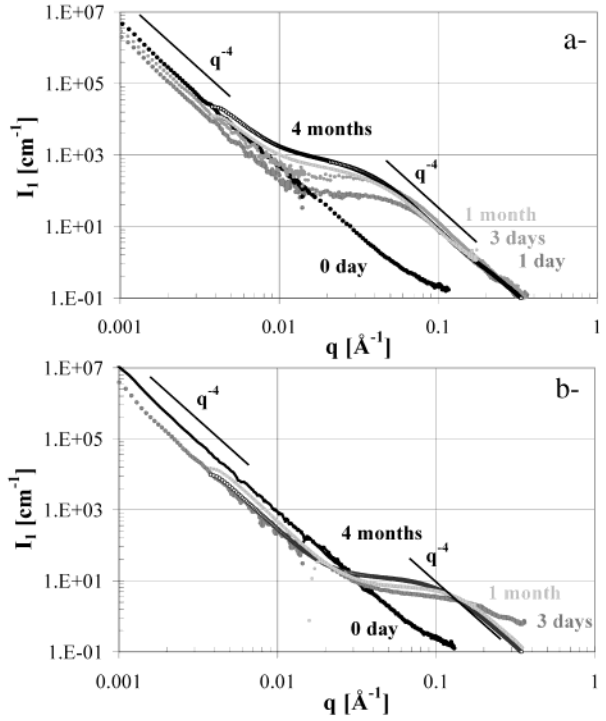

Figure 3. Small-angle X-ray scattering patterns of the glasses containing (a) 0.5% ZrO_2 and (b) 5% ZrO_2, nonaltered and altered for 1 day, 3 days, 1 month, and 4 months.

the loss of silicon at saturation is very similar for these two samples. This must result in a difference in the morphology of the alteration layer.

3.2. Morphology of the Altered Layer. The intensity scattered by two glasses altered for various times is shown in Figure 3. As explained in the Experimental Section (2.4), the intensity $I_1(q)$ is expressed per unit volume of solid. The use of a scaled intensity enables a qualitative and quantitative comparison of the SAXS patterns.

First, the patterns of the glass containing 0.5% ZrO_2 (nonaltered and altered for 1 day, 3 days, 1 month, and 4 months) are given in Figure 3a. The nonaltered glass follows a Porod law[23] (straight line with q^{-4} behavior) on a large q scale (until $q = 0.04$ Å^{-1}). Here, this behavior is the signature of a smooth and sharp interface between the external envelope of the particles and water. The absence of any other contribution to the signal indicates that the glasses are homogeneous down to the scale of 1 nm. Upon alteration, the shape of the scattering curve becomes very different. Indeed, the same Porod law is observed at low q values but on a smaller q scale (until $q = 0.01-0.02$ Å^{-1}). The amplitude of this Porod limit decreases with the alteration time, indicating that the difference in electronic density between the particles and water diminishes. Moreover, at higher q values, another Porod law can be attributed to the creation of a large surface area and to the presence of pores[21] whose characteristic size is in the nanometer range. This signal cannot arise from the formation of ZrO_2 nodules.[17] Indeed, an anomalous small-angle X-ray scattering experiment was previously carried out on these glasses.[17] The shape of the curves obtained at different energies near the K edge of Zr was identical. Only a translation of the curves was observed because of the different electronic density of Zr. Consequently, the hypothesis of the precipitation of nodules of ZrO_2 or of a mixture of ZrO_2 and SiO_2 was rejected, and the chemical composition layer was considered to be homogeneous. From a kinetics point of view, the difference in shape between the patterns of the nonaltered glass and the glass altered for 1 day is striking. This indicates that the glass particles are already highly altered after only 1 day, which is a confirmation of the results of the chemical analysis. For longer alteration times, the shape and intensity of the patterns evolve gradually: a slow evolution of the porosity exists.

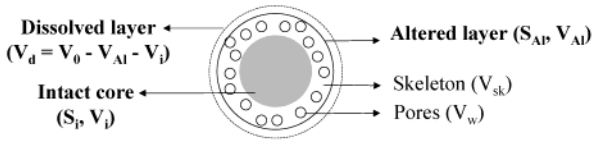

Figure 4. Schematic representation of an altered glass particle. S_i corresponds to the interface between the intact core and the altered layer; S_{Al} is the surface area of the altered layer. V_i is the volume of the intact core; V_{Al} is the total volume of the altered layer, and V_w and V_{sk} correspond to the volumes of the pores and the skeleton, respectively, in this altered layer. V_d is the volume of the totally dissolved superficial layer.

The results obtained for a glass containing more zirconia (5%) are very similar at first sight (Figure 3b) but with a much slower evolution as for the chemical analysis. Besides, the second Porod limit begins at higher q values, which means that the pores are smaller. For the sample altered for 3 days, this regime cannot be obtained. This means that the interface between pores and water is rough.

The most important point within this description of the SAXS patterns is certainly the fact that a Porod law is observed at high q values when the glass particles are altered. As already mentioned, this is proof that a smooth and sharp interface exists between the pores and the skeleton of the altered layer (except for 3 days in the 5% ZrO_2 case). The altered layer can thus be described as a real nanoporous medium. This also allows us to analyze the SAXS patterns quantitatively as follows.

4. Discussion

4.1. Hypothesis and Definitions of the Altered Glass. We now propose a model to analyze the results of both chemical and SAXS experiments. It is based on the idea that the glass is altered simultaneously through the dissolution (shrinkage) of its outer envelop and the growth of a porous altered layer as schematized in Figure 4. The pristine glass particles present a total surface S_0 and occupy a volume V_0. After alteration, the particles consist of an intact core (of surface S_i and volume V_i) surrounded by a porous layer. The core has the same composition and density as the pristine glass. The superficial layer is made of a solid skeleton (with composition and density d_{sk} different from those of the pristine glass) and of pores filled with solvent. It is considered to be a chemically homogeneous medium, which has been totally depleted in the soluble elements (Na and B) and from which part of the Si has also been removed. This assumption is based on previous SIMS studies[8,22] that have shown that the altered layer is thoroughly emptied of the Na and B elements. The same studies have shown that, on the scale of our analysis, relatively sharp glass-altered layer−water interfaces can be considered. The layer is characterized by its internal surface S_{Al}, which corresponds to the interface between the skeleton and the pores, by its global volume V_{Al}, and by the volume of the pores V_w and of the skeleton V_{sk}. A fraction of the particle can also be totally dissolved so that the external particle size shrinks. The dissolved volume will be noted as V_d ($V_d = V_0 - V_{Al} - V_i$), and we will define the contraction fraction as $\Phi_d = V_d/V_0$.

The alteration process can be characterized, from a global point of view, by the volume fractions:

$$\text{of the intact core: } \Phi_i = \frac{V_i}{V_0}$$

$$\text{of the altered layer: } \Phi_{Al} = \frac{V_{Al}}{V_0}$$

$$\text{of the dissolved layer: } \Phi_d = \frac{V_d}{V_0} = 1 - \Phi_i - \Phi_{Al}$$

However, the specific surface area ($\Sigma = S_{Al}/V_{Al}/d_{sk}$) and the specific porous volume ($\phi = V_w/V_{Al}$) are intrinsic parameters related to the altered layer that describe its morphology.

In the following text, we describe a method, already developed in detail elsewhere,[17] to determine all of these parameters. It couples the results of the chemical analysis in solution and the general SAXS theorems (Porod limits and invariant).

First, the chemical analysis allows us to calculate the mass of skeleton in the altered layer and the fraction of intact core Φ_i. Our experiments show that Na and B are the most soluble elements and that they are removed to the same extent, although a slightly larger amount of B is leached. This is probably because Na is retained in the glass as a counterion of Si−O$^-$ or Zr−O$^-$. Thus, the boron loss can be used as the alteration tracer (i.e., it allows us to calculate the maximum depth of alteration).

The fraction of intact core Φ_i is then simply obtained by eq 4:

$$\Phi_i = 1 - \mathrm{LF(B)} \tag{4}$$

Moreover, the mass of each cation j in the skeleton of the altered layer is proportional to the initial mass of j in the pristine glass ($m_0(j)$):

$$m(j) = m_0(j)[\mathrm{LF(B)} - \mathrm{LF}(j)] \tag{5}$$

The mass of skeleton in the altered layer can then be easily deduced from the molar mass of the oxide $M(jO_x)$ associated with the element j of molar mass $M(j)$:

$$m_{sk} = \sum_j m(j)\frac{M(jO_x)}{M(j)} \tag{6}$$

However, the volume fraction of the skeleton Φ_{sk} cannot be deduced from this expression because the density of the skeleton d_{sk} is not known. The volume fraction of the pores Φ_w is also unknown. Consequently, the volume fraction of the altered layer $\Phi_{Al} = \Phi_w + \Phi_{sk}$ cannot be determined. These values can still be obtained from the quantitative analysis of the SAXS patterns, using the general theorems of X-ray scattering (Porod limit and invariant).[23]

At small q values (corresponding to large sizes), the scattered intensity is related to the electronic contrast at the two interfaces: intact glass−altered layer and altered layer−water. The intensity obeys the Porod law, characteristic of smooth interfaces, $I(q) = P_s\, q^{-4}$, where it can be demonstrated that the P_s coefficient is related to the characteristics of the altered layer:[17]

$$P_s = 2\pi\frac{S_0}{V_0}\frac{(\Phi_i + \Phi_{Al})^{2/3}}{\Phi_i + \Phi_{Al} - \phi\Phi_{Al}} \times \left[\frac{\Phi_i}{\Phi_i + \Phi_{Al}}(\rho_{Al} - \rho_i)^2 + (\rho_{Al} - \rho_w)^2\right] \tag{7}$$

where ρ_{Al}, ρ_i, and ρ_w are the electronic densities of the altered layer, of the intact core, and of water, respectively. Because Φ_i has already been calculated from the chemical analysis, the only unknown parameters in this expression are Φ_{Al}, ϕ, and ρ_{Al}. Their values cannot be calculated without assuming the values of d_{sk} and V_w. At this stage, one has the choice of setting d_{sk} equal to the amorphous silica density or of following a more complete procedure as described below to obtain self-consistent d_{sk} and V_w. The second solution was chosen.

Indeed, a second relation can be obtained by the invariant theorem. Subtracting the intensity scattered by the macroscopic interface discussed above yields information about the porous volume in the altered layer. Thus, the invariant can be written as follows:[17]

$$\mathrm{INV} = \int_0^\infty (I_1 - P_s)q^2\,dq = 2\pi^2(\rho_{sk} - \rho_w)^2(1 - \phi)\frac{\phi\Phi_{Al}}{\Phi_i + \Phi_{Al} - \phi\Phi_{Al}} \tag{8}$$

where ρ_{sk} (electronic density of the solid skeleton in the altered layer) can be calculated using the value assumed for d_{sk}.

Consequently, the quantitative analysis consists of varying the two parameters, d_{sk} and V_w, until reaching a consistency between the values of P_s and INV measured by SAXS and those calculated by eqs 7 and 8. This allows us to determine Φ_{Al}, Φ_d, and ϕ.

Finally, at large q (corresponding to small distances), a Porod law is again observed (Figure 3), and the scattered intensity corresponds to the electronic contrast at the interface between the skeleton and water in the pores of the altered layer. The amplitude P_L of this Porod law, $I(q) = P_L.q^{-4}$ is related to the specific surface area Σ of the altered layer:

$$P_L = \lim_{q\to\infty}(I_1 q^4) = 2\pi d_{sk}\Sigma\frac{\phi_{Al}}{1 - \phi\phi_{Al}}(\rho_{sk} - \rho_w)^2 \tag{9}$$

4.2. Morphology of the Altered Glass Particles. The macroscopic parameters (i.e., the volume fraction of the intact core (Φ_i), of the altered layer (Φ_{Al}), and of the dissolved layer (Φ_d)) are presented in Figure 5. In this schematic view, the pristine glass corresponds to 100%. The proportions of the intact core (in black), altered layer (in pale gray), and dissolved layer (in white) can be visualized for the six compositions at three different alteration times. The results are given for 3 and 15 days and also for 4 months to characterize the long-term alteration. The results for the glasses containing 5 and 10% ZrO_2 after 3 days of alteration are not given. Indeed, a Porod law at high q values cannot be clearly defined within the q scale of the experiment.

First, as a consequence of the observations of the B leaching, the proportion of the intact core decreases with increasing % ZrO_2 from 0 to 1% and then increases when adding more ZrO_2 to the glass.

Second, the particle size decreases with time for the glasses containing 0 to 1% ZrO_2: for example, for the glass containing no zirconium, Φ_d increases from 10% after 1 day to 30% at saturation. In the meantime, Φ_{Al} is nearly constant. This indicates that the alteration front moves forward at a constant alteration volume and that the alteration progresses by further dissolution of the particle surfaces. On the contrary, the particle size of the glasses containing more than 2% ZrO_2 remains constant, and the altered volume increases for the particles that cannot contract.

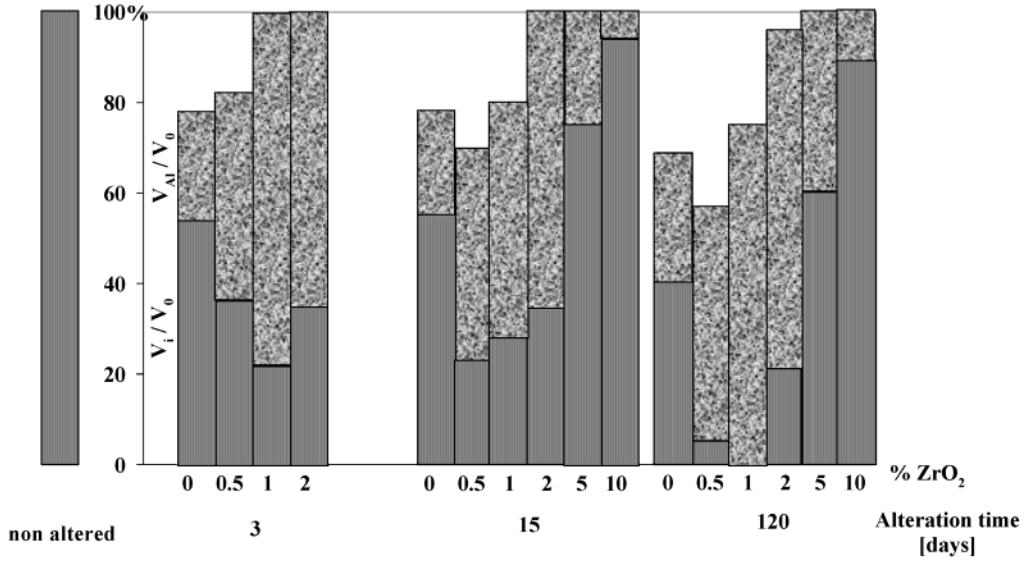

Figure 5. Representation of the proportion of the intact core volume (V_i/V_0, in black) and of the altered layer volume (V_{Al}/V_0, in gray) for the different glasses after three alteration times: after 3, 15 and 120 days.

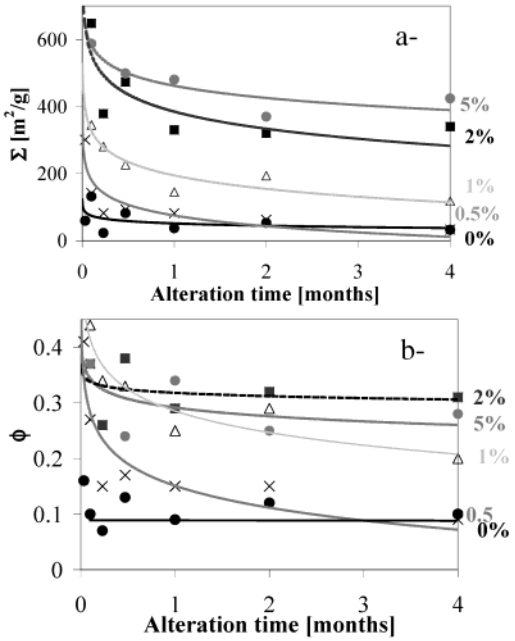

Figure 6. Evolution of (a) the specific surface area Σ (surface of the altered layer S_{Al} to the volume of the altered layer V_{Al} and to the density of the skeleton d_{sk}) and (b) the ratio of the specific porous volume fraction ϕ (volume of pores V_w to volume of the altered layer V_{Al}) vs the alteration time for the glasses containing 0% (●), 0.5% (×), 1% (△), 2% (■), 5% (gray ●).

The morphology of the altered layer can be described by its intrinsic parameters, Σ and ϕ, the evolutions of which are given in Figure 6a and b, respectively, and in Table 3. They describe the layer porosity. The glass containing 10% ZrO_2 is not represented in these Figures. Indeed, the altered layer is very thin, and its porosity cannot be obtained with accuracy. For all of the glasses, a very large specific surface area and porous volume are created within the first few days (between 50 and 500 m^2/g and 0.1 to 0.45, respectively). The addition of Zr to the glass results in a large increase of both Σ and ϕ (Figure 6b).

From a kinetics point of view, no evolution of Σ can be detected (taking into account the scatter of data) for the glass containing no zirconium because the alteration is very rapid.

TABLE 3: Specific Surface Area Σ and Porous Volume ϕ of the Altered Layer of the Altered Glasses after 3 Days and 4 Months

alteration time	3 days		4 months	
	Σ[m^2/g]	ϕ	Σ[m^2/g]	ϕ
0% ZrO_2	132	0.1	32	0.10
0.5% ZrO_2	142	0.27	33	0.09
1% ZrO_2	345	0.44	118	0.20
2% ZrO_2	648	0.37	320	0.32
5% ZrO_2	588	0.37	370	0.28

For the other glasses, the specific surface area clearly decreases as the alteration proceeds. The evolution of ϕ with the alteration time is weaker but still decreases with time.

4.3. Alteration Mechanism and Effect of Zirconium. The main results of the chemical analysis and SAXS experiments are the following: First, a porous superficial layer is created upon alteration by water. This results in the formation of a large specific surface area (Σ) and porous volume (ϕ) created within the first day of alteration for all of the glasses. Second, the values of Σ and ϕ decrease as the alteration proceeds. It is also observed that these two parameters are higher for increasing amounts of ZrO_2. Third, the glasses containing less than 2% ZrO_2 undergo shrinkage and the altered volume is constant, whereas the Zr-rich glasses do not contract and the volume of the altered layer increases with time.

Considerations common to all the glasses concerning the aging of the altered layer will be addressed first. Second, the role of zirconium on the alteration will be discussed. In particular, the addition of zirconium has a strong influence on the morphology of the altered layers.

The main guide of the analysis is that the morphology of the altered layer and the dissolution of elements are intrinsically linked. Indeed, a common feature for all of the glasses is the formation, in the first few days of alteration, of a superficial porous layer. This layer does not appear to be a branched fractal network such as those obtained during the sol−gel process,[24] as assumed for a long time. This layer is made of two bulk media (solid and water), and a true interface between them can be defined as revealed by the Porod behavior in SAXS. As a first approximation, the pores can be considered to be due to the leaching of sodium, boron, and silicon. Nevertheless, the leaching of simple entities such as B_2O_3 and Na_2O would leave

a residual porosity of a few angstroms only. Consequently, a rearrangement of the skeleton through dissolution−recondensation of the less soluble species (SiO_2 and ZrO_2) is necessary to explain a characteristic pore size of a few nanometers. The dissolution−recondensation process can be further supported by the following point: for the three glasses containing 0, 0.5, and 1% ZrO_2, part of the glass is totally dissolved during the alteration, and LF(B) is equal to the sum of the volume fraction of the altered layer Φ_{Al} and of the dissolved layer Φ_d (Figure 5). The chemical analysis indicates that LF*(Si) $\approx$ 20% at saturation (Figure 2). But in the SAXS analysis, the fraction of dissolved layer Φ_d is equal to 30, 40, and 20% (for 0, 0.5, and 1% ZrO_2, respectively). Consequently, Φ_d is always higher than LF*(Si), again supporting the hypothesis that part of the silicon that has been dissolved from the glass skeleton recondenses deeper in the altered layer. The recondensation of silica further results in a densification of the altered layer, which explains the decrease of the specific porous volume when the alteration proceeds beyond the pore nucleation stage. Our analysis is similar to that of Tomozawa et al., who considered that the leaching of soluble Na, B, and Si species leaves a hydrated glass that yields a phase separation of water and silica.[25] The recondensation of silica at saturation probably forms a blocking layer that stops the alteration. This effect was first observed by numerical Monte Carlo simulations.[11,12] The results described above are common to all of the glasses. However, the addition of zirconium leads to differences in the mechanisms of aging:

(i) The addition of Zr has a strong influence on the dissolution kinetics, but it also affects the global shape of the altered grain. For the glasses containing less than 2% ZrO_2, a decrease of the particle size is observed, whereas the dissolution of the superficial part of the glass is impossible for the glasses containing more than 2% ZrO_2. This can be explained by the fact that zirconium is quasi-insoluble. Moreover, the solubility of silicon atoms attached to zirconium atoms is also probably very low. Thus, the presence of ZrO_2 reinforces the skeleton of the glass and does not permit the complete dissolution of the glass. In this case, the evolution is characterized by the increased thickness of the altered layer.

(ii) The addition of ZrO_2 simultaneously induces a larger specific surface area and smaller pores. Another indication of this result is to calculate the ratio $^{3\phi}/_{\Sigma}$. Indeed, in a very crude approximation, considering spherical pores, it is proportional to the radius of these pores. This ratio decreases from 4 to 2 nm when adding 0 to 10% ZrO_2. This result, also observed in other glass compositions,[26] is due to the low solubility of zirconium which both inhibits a complete rearrangement of the skeleton and offers a very good recondensation site for silica. Thus, the large specific area of the resulting altered layer delays the formation of dense silica blocking the alteration. Indeed, when Σ increases, the recondensation of silica is spread out on a wide surface and is less efficient at reorganizing the porous structure and passivating the glass alteration. Consequently, the glasses containing 0.5 and 1% ZrO_2 are altered down to the center ($\Phi_i \approx 0$). For higher zirconium contents, the low solubility of silicon imposed by the Zr−O−Si bonds becomes the predominant factor, as revealed by the low concentration of Si at saturation, and the alteration depth decreases accordingly.

5. Conclusions

By coupling chemical analysis and SAXS measurements, it was possible to describe the mechanisms of alteration of simplified glasses and the effect of an element of low solubility, Zr in this case. A general observation is that the first day the majority of different elements (Na, B and Si) dissolve and a large surface and porous volume are created. The presence of nanoporosity was attributed to a rearrangement of the skeleton of the altered layer by the dissolution−recondensation of silica and zirconia. Then, a ripening of the pores is observed as the alteration proceeds. A distinction in terms of morphology has to be made between the glasses containing less than 2% ZrO_2 and those containing more than 2%. Indeed, the reactivity of silicon depends on its link with zirconium, which is an insoluble element. For the group with low Zr content, a fraction of the altered-layer skeleton can be totally dissolved so that the particles can decrease in size. In this case, the alteration proceeds by a dissolution of the particles rather than by an increase of the altered-layer volume. In the second case, more silicon atoms become insoluble; consequently, it is impossible to dissolve a part of the skeleton entirely. As a consequence, the particle size remains the same, and the altered volume increases.

References and Notes

(1) Bange, K.; Anderson, O.; Rauch, F.; Lehuédé, P.; Radlein, E.; Tadokoro, N.; Mazzoldi, P.; Rigato, V.; Matsumoto, K.; Farnworth, M. *Glastech. Ber.***2001**, *74*, 5.
(2) Buchmeier, W.; Jeschke, P.; Sorg, R. *Glastech. Ber.***1996**, *769*, 159.
(3) Libourel, G.; Barbey, P.; Chaussidon, M. *Recherche* **1994**, *722*, 168.
(4) Techer, I.; Advocat, T.; Lancelot, J.; Liotard, J.-M. *J. Nucl. Mater.* **2000**, *282*, 40.
(5) Techer, I.; Advocat, T.; Lancelot, J.; Liotard, J.-M. *Chem. Geol.* **2001**, *176*, 235.
(6) Hench, L. L.; Clarck, D. E. *J. Non-Cryst. Solids* **1978**, *28*, 83.
(7) Bunker, B. C.; Arnold, G. W.; Day, D. E.; Bray, P. J. *J. Non-Cryst. Solids* **1986**, *87*, 226.
(8) Vernaz, E.; Gin, S.; Jégou, C.; Ribet, I. *J. Nucl. Mater.* **2001**, *298*, 27.
(9) Grambow, B.; Müller, R. *J. Nucl. Mater.* **2001**, *298*, 112.
(10) Donzel, N.; Gin, S.; Augereau, F.; Ramonda, M. *J. Nucl. Mater.* **2003**, *317*, 83.
(11) Devreux, F.; Barboux, P.; Filoche, M.; Sapoval, B. *J. Mater. Sci.* **2001**, *36*, 1331.
(12) Devreux, F.; Ledieu, A.; Barboux, P.; Minet, Y. Submitted to *J. Non-Cryst. Solids*.
(13) Santra, S.; Sapoval, B.; Barboux, P. *Europhys. Lett.* **1998**, *41*, 297.
(14) Fillet, S.; Phalippou, J.; Zarzycki, J.; Nogues, J. L. *J. Non-Cryst. Solids* **1986**, *82*, 232.
(15) Walter, G.; Kranold, R.; Enke, D.; Goerigk, G. *J. Appl. Crystallogr.* **2003**, *36*, 592.
(16) Deruelle, O.; Spalla, O.; Barboux, P.; Lambard, J. *J. Non-Cryst. Solids* **2000**, *261*, 237.
(17) Spalla, O.; Barboux, P.; Sicard, L.; Thill, A.; Lyonnard, S.; Bley, F. submitted to *J. Non-Cryst. Solids*.
(18) Moltchanova, O. S. *Steklo y Keram.* **1957**, *14*, 5.
(19) Zemb, T.; Taché, O.; Né, F.; Spalla, O. *Rev. Sci. Instrum.* **2003**, *74*, 2456.
(20) Lambard, J.; Lesieur, P.; Zemb, T. *J. Phys. I* **1992**, *2*, 1191.
(21) Spalla, O.; Lyonnard, S.; Testard, F. *J. Appl. Crystallogr.* **2003**, *36*, 338.
(22) Lodding, A.; Van Iseghem, P. *J. Nucl. Mater.* **2001**, *298*, 197.
(23) Glatter, O.; Kratky, O. *Small-Angle X-ray Scattering*; Academic Press: London, 1982.
(24) Schaeffer, D. W.; Keefer, K. D. *Phys. Rev. Lett.* **1986**, *56*, 2199.
(25) Tomozawa M.; Cappella, S. *J. Am. Ceram. Soc.* **1983**, *66*, C-24.
(26) Du, W. F.; Kuraoka, K.; Akai, T.; Yazawa, T. *J. Phys. Chem. B* **2001**, *105*, 11949.